Analyst

PAPER

View Article Online
View Journal

Cite this: DOI: 10.1039/c8an02194e

Optimizing peptide nucleic acid probes for hybridization-based detection and identification of bacterial pathogens†

Kathleen E. Mach, [a,b] Aniruddha M. Kaushik,[c] Kuangwen Hsieh,[c] Pak Kin Wong,[d] Tza-Huei Wang[c] and Joseph C. Liao*[a,b]

Received 14th November 2018,
Accepted 9th January 2019

DOI: 10.1039/c8an02194e

rsc.li/analyst

Point-of-care (POC) diagnostics for infectious diseases have the potential to improve patient care and antibiotic stewardship. Nucleic acid hybridization is at the core of many amplification-free molecular diagnostics and detection probe configuration is key to diagnostic performance. Modified nucleic acids such as peptide nucleic acid (PNA) offer advantages compared to conventional DNA probes allowing for faster hybridization, better stability and minimal sample preparation for direct detection of pathogens. Probes with tethered fluorophore and quencher allow for solution-based assays and eliminate the need for washing steps thereby facilitating integration into microfluidic devices. Here, we compared the sensitivity and specificity of double stranded PNA probes (dsPNA) and PNA molecular beacons targeting *E. coli* and *P. aeruginosa* for direct detection of bacterial pathogens. In bulk fluid assays, the dsPNAs had an overall higher fluorescent signal and better sensitivity and specificity than the PNA beacons for pathogen detection. We further designed and tested an expanded panel of dsPNA probes for detection of a wide variety of pathogenic bacteria including probes for universal detection of eubacteria, *Enterobacteriaceae* family, and *P. mirablis*. To confirm that the advantage translated to other assay types we compared the PNA beacon and dsPNA in a prototype droplet microfluidic device. Beyond the bulk fluid assay and droplet devices, use of dsPNA probes may be advantageous in a wide variety of assays that employ homogenous nucleic acid hybridization.

Introduction

Accurate, timely diagnosis is key to efficacious treatment of infectious diseases. Particularly for acute bacterial infections, point of care (POC) devices capable of distinguishing whether a patient has an infection, determining the causative pathogenic species, and directing the appropriate treatment can improve patient outcomes and promote antibiotic stewardship.[1–5] Because the current diagnostic standard of culture and antimicrobial susceptibility testing (AST) requires 2–4 days to provide this objective information, there are strong interests to develop devices to expedite pathogen detection and characterization.[6]

Nucleic acid detection is an integral part of many new approaches to rapid pathogen diagnosis.[7–10] PCR and related target amplification techniques, while highly sensitive, may require complex sample preparation steps to remove amplification inhibitors and require several hours from sample to answer. PCR may be a good option for pathogen detection in typically sterile environments such as cerebral spinal fluid and blood where the presence of any bacteria can indicate serious infection, however other samples types such as sputum or urine can be prone to false positive results due to contamination during sample collection with normal flora.[11] Alternatively, amplification-free detection is commonly achieved through direct hybridization of linear DNA oligonucleotide probes labeled with enzymes or fluorescent tags.[12,13] The use of oligonucleotide probes with a single label typically requires that the target sequence be immobilized on a solid support for hybridization so excess unbound probe can be washed away.

Dual label probes such as molecular beacons are a good alternative for homogenous sensors. Molecular beacons are

[a]Department of Urology, Stanford University School of Medicine, Stanford, CA, USA. E-mail: jliao@stanford.edu; Tel: +1 650-852-3284
[b]Veterans Affairs Palo Alto Health Care System, Palo Alto, CA, USA
[c]Departments of Mechanical Engineering and Biomedical Engineering, Johns Hopkins University, Baltimore, MD, USA
[d]Department of Biomedical Engineering, The Pennsylvania State University, University Park, PA, USA

†Electronic supplementary information (ESI) available. See DOI: 10.1039/c8an02194e

single-stranded probes designed with a fluorophore and a quencher at opposing ends. For DNA molecular beacons the fluorophore and quencher are kept in close proximity through short complimentary regions at either end of the probe. In the case of peptide nucleic acids beacons, hydrophobic interactions keep the labeled ends in close proximity.[14] Double stranded probes with a fluorophore label on one strand and a shorter complimentary sequence with a quencher can function similarly to the beacon.[15,16] In the unbound state for both beacons and double stranded probes, the fluorophore and quencher are adjacent resulting in little to no fluorescent signal. Hybridization of the target sequence displaces the quencher either through opening of the probe or competitive binding with the quencher sequence allowing the probe to fluoresce and detection of the hybridization (Fig. 1). Both molecular beacons and double stranded probes are especially amenable to system integration in molecular diagnostics as they simplify sample preparation through elimination of additional washing steps for removal of excess probe and allow for solution-based hybridization.[17]

Molecular beacon or double stranded probes based on PNAs offer several advantages over DNA probes.[18] PNAs are a hybrid between protein and nucleic acid with a polyamine backbone and nucleotide residues.[19] PNAs can form stable hybridization complexes with DNA and RNA molecules through standard Watson–Crick base pairing.[20] Since PNA is neither fully peptide nor nucleic acid the molecule is resistant to nucleases and proteases and is thermostable.[21] The neutral backbone of PNAs increase the hybridization rate as electrostatic forces that limit DNA/DNA and DNA/RNA hybridization are no longer a factor. Also, hybridization with PNA probes is less susceptible to salt concentration and well suited for direct applications using clinical samples. The more stable PNA/DNA or PNA/RNA complexes have a higher melting temperature (T_m) and a greater difference in T_m with mismatched sequences improving specificity compared to DNA probes.[22,23]

Detection of bacterial ribosomal RNA (rRNA) is often used for specific probe based molecular pathogen identification and monitoring of growth.[24,25] As one of the most abundant molecules with 15 000 to 70 000 copies per bacterial cell, detection of rRNA allows for sensitive detection without target amplification.[26–28] The 16S rRNA molecule is also one of the best-characterized molecules with thousands of sequences available for *in silico* analysis of candidate probe specificity.[29–31] Common sequences between bacterial species allow for universal or group detection through probes targeting conserved regions, while species-specific sequences allow for refined pathogen identification. As such, several probes have been described in the literature for use in molecular diagnostics that can be adapted to a variety of applications. In particular, fluorescence *in situ* hybridization (FISH) targets 16S rRNA with a wide variety of probe configurations including single stranded DNA (ssDNA) and PNA beacons, and double stranded DNA (dsDNA) and PNA probes.[32,33] One commercially available clinical microbiology test, QuickFISH (OpGen), uses dsPNA for rapid detection of pathogens from blood culture.[32] While this approach still requires an initial overnight incubation of the patient sample, it has been shown to reduce pathogen identification step to about 30 minutes from positive blood culture.

Droplet microfluidic systems have recently emerged as a powerful tool for high-throughput analysis with exceptional sensitivity through encapsulation of single molecules or cells within monodisperse droplets.[34–38] These systems can be used to discretize samples containing bacterial pathogens into

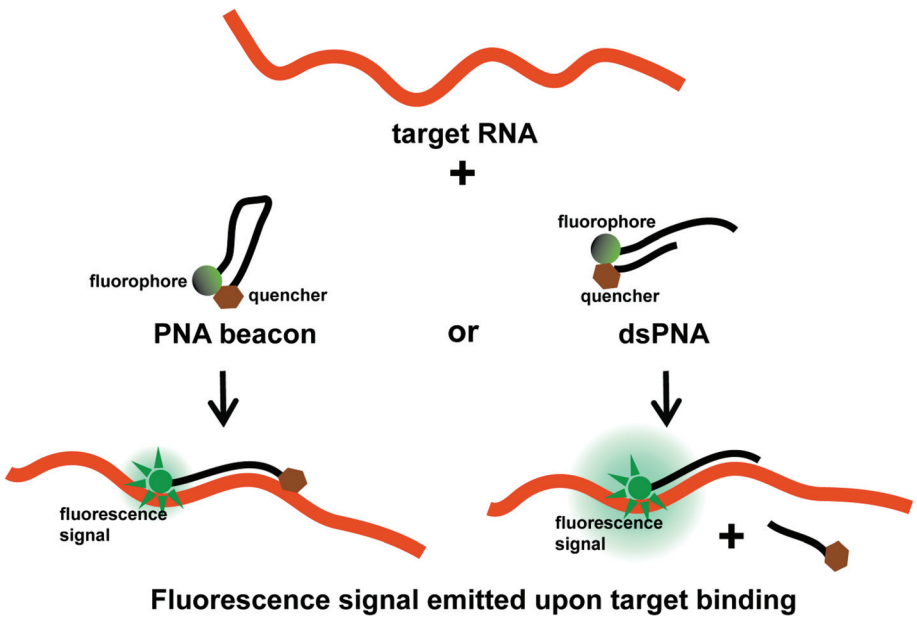

Fig. 1 Fluorescent detection of nucleic acid with beacon and double stranded probes. Target binding dissociates the quencher and fluorophore either through strand opening in PNA beacon or strand displacement in dsPNA probes.

thousands to millions of picoliter (pL) droplets, each of which serves as an isolated reaction chamber containing 1 or 0 bacterial cells.[39–41] Confinement of single cells in pL droplets results in a high effective concentration of nucleic acids that can increase sensitivity of detection and obviate the need for PCR amplification.[41] As such, the single-cell sensitivity afforded by droplet platforms can facilitate drastically improved limits of detection compared to bulk detection. Further, the digital readout from droplet microfluidic systems can allow for more accurate quantitation of bacteria.

Since a key determinant of sensitive and specific pathogen detection in nucleic hybridization assays is the labeled probe, we directly compared the sensitivity and specificity of PNA beacons and dsPNA probes for pathogen identification. Here we report that dsPNAs have better sensitivity and specificity than PNA beacons targeting the same sequence in our assays. We initially compared the probe configuration in a bulk (100 μl) fluid assay then demonstrated that the advantage of the double stranded probe held true when the probes where used for pathogen detection in a droplet microfluidic system. Our findings may be generalizable for other homogeneous hybridization detection strategies and the probes adaptable to a wide variety of devices.

Methods

Probes and bacterial culture

The pathogen detection probes designed to target all bacteria, *Enterobacteriaceae* family, *E. coli, P. aeruginosa* and *P. mirabilis* 16S rRNA and the universal probe were based on previous reports.[42–45] Probe sequences are reported in Table 1. All PNA sequences were synthesized by PNA Bio (Newbury Park, CA) and DNA quencher sequences were synthesized by Integrated DNA Technologies (San Diego, CA).

Uropathogenic *E. coli* (UPEC) strain (CFT073) was purchased from ATCC (Manassa, VA.) All other strains are uropathogenic clinical isolates from the Palo Alto VA clinical microbiology laboratory. For bulk pathogen detection experiments, bacteria were grown in cation adjusted Muller-Hinton (MH) media at 37 °C in a shaking incubator (Excella E24, New Brunswick Scientific) to mid-log phase and diluted as appropriate. For droplet assays, *E. coli* was cultured and stored at −80 °C until assayed.

Bulk fluid pathogen detection

For pathogen detection, probes were diluted in 2× hybridization buffer (50 mM Tris pH8, 100 mM NaCl, 1% PVP, 10 mM EGTA) to desired concentration and 25 μl of probe was mixed with an equal volume of media or culture for a final concentration of 25 mM Tris pH8, 50 mM NaCl, 0.5% PVP, 5 mM EGTA, 50% MH media or culture. Final probe and bacteria concentrations are indicated in results. For dsPNA probes the DNA quencher sequence was in three-fold molar excess of the labeled PNA. The probe/bacteria mix was heated to 95 °C for 2 min to thermolyse the bacteria followed by incubation at 60 °C for 30 min to allow for probe hybridization. To control incubation time and temperature, 95 °C and 60 °C incubations were carried out in at thermocycler (Eppendorf Mastercycler). Immediately after hybridization fluorescence was measured in a fluorescence microplate reader (Molecular Dynamics SpectraMax) at excitation wavelength 492 nm and emission wavelength 518 nm.

Microfluidic device design and fabrication

The microfluidic device design consists of a 10 μm flow-focusing nozzle for droplet generation and a 10 μm channel constriction for droplet detection. The droplet generation and droplet detection channels of the device are connected by a ~30 cm Tygon tubing (Cole-Parmer) with an inner diameter of approximately 500 μm. In order to fabricate the microfluidic device, a casting mold was created by spinning a 20 μm layer of SU8-3050 photoresist (MicroChem) onto a 4 inch silicon wafer and patterned using standard photolithography. The microfluidic devices were made of polydimethylsiloxane (PDMS) by pouring 50 g of 10 : 1 ratio of Sylgard 184 (Dow Corning) base to curing agent onto the SU8 mold. The PDMS device was then permanently bonded to cover glass (130 μm thickness, Ted Pella) through oxygen plasma treatment in order to seal the channels. Prior to device operation, the microfluidic chips were treated with Aquapel and baked at

Table 1 dsPNA probe sequences

	Sequence	Length	Target
UNI339	GCTGCCTCCCGTAGGA-K-FAM	16	Eubacteria
	GGAGGGCATCCT-IABk	12	
EC467	FAM-O-TCAATGAGCAAAGGT-KK	15	*E. coli*
	IABk-AGTTACTCGT	10	
PA584	FAM-O-AACTTGCTGAACCAC	15	*P. aeruginosa*
	IABk-TTGAACGACT	10	
EB1272	FAM-O-TATGAGGTCCGCTTG	15	Enterobacteriaceae
	IABk-ATACTCCAGG	10	
PM1014	FAM-O-TCCTCTATCTCTAAAGG	17	*P. mirabilis*
	IABk-AGGAGATAGAG	11	

For each probe sequence, top line is the fluorophore labeled PNA and bottom is DNA quencher. E = glutamate, K = lysine, O = linker sequence, FAM = fluorescein, IABk = Iowa black quencher.

80 °C for at least 20 minutes to render microfluidic channel surfaces hydrophobic.

Microfluidic device operation and droplet fluorescence detection

Prior to droplet generation, stock *E. coli* (ATCC 25922) was thawed, washed twice, and diluted to 4×10^7 cfu mL^{-1} in in either hybridization buffer or MH media. Separately, *E. coli* probes at 200 nM PNA beacon or 200 nM dsPNA and 600 nM quencher were diluted in hybridization buffer. Bacterial solution and probes solution were then introduced into separate sections of Tygon tubing. Both sections of Tygon tubing were individually connected to Hamilton 1000 glass syringes (Sigma-Aldrich) containing FC-40 oil (Sigma-Aldrich). FC-40 in the syringe was used to push the aqueous samples from Tygon tubing into the device using a syringe pump (Harvard Apparatus). BioRad QX200 Droplet Generation Oil was introduced into the oil inlet of the device by a separate syringe pump. A flow rate of 20 μL h^{-1} was used for both aqueous phases, while 60 μL h^{-1} was used for the oil phase. In order to confirm stable and uniform droplet generation, the device was imaged using a 4× objective lens and a CCD camera during droplet generation and after droplet incubation. Lysis and hybridization were conducted as the droplets flowed through the Tygon tube connecting the droplet generation and droplet detection regions of the microfluidic device. Importantly, separate lengths of the Tygon tube were clamped onto a 95 °C Peltier heater and a 60 °C Peltier heater, such that all droplets were subject to 2 min at 95 °C followed by 30 min at 60 °C as in the bulk fluid assay. Continuous-flow droplet detection was conducted using a custom designed optical stage consisting of a 488 nm laser excitation source (OBIS, Coherent, Inc.) and a silicon avalanche photodiode detector (APD) (SPCM-AQRH13, ThorLabs). The laser was operated at 4 mW power and was focused into the detection zone of the device using a 40× objective (Thorlabs RMS40X-PF, NA 0.75, focal depth approximately 0.6 μm). As droplets flowed through the custom laser-induced fluorescence detection zone, fluorescence data was continuously acquired and recorded using the APD with 0.1 ms sampling time. A custom-built LabVIEW program was used for fluorescence data acquisition.

Laser induced fluorescence data analysis

A custom MATLAB program was developed for analyzing the raw fluorescence intensity data acquired from the APD. From the fluorescence intensity time trace of each experimental run, the program looks for individual droplets by quantifying peak widths and peak heights. Once droplet position and fluorescence intensity are identified for all droplets in a sample, we plot the intensities as a histogram with 150 bins. Resulting histograms typically follow a bimodal distribution, and in order to classify the respective subpopulations, we fit the first droplet histogram peak (the empty droplet or "background" subpopulation) with a Gaussian curve. Based on the fitted curve, we calculate the mean intensity of the empty droplet population as well as the standard deviation. All droplets whose intensities are 3 standard deviations above the empty droplet mean intensity are classified as bacteria-containing "positive droplets." Signal to background ratios are calculated by dividing the mean intensity of positive droplets by the mean intensity of background droplets.

Results

The PNA probe sequences targeting *E. coli*[45] and *P. aeruginosa*[43] used in this study were in previously described FISH assays. However, in the prior assays the probes were labeled with a single fluorophore and unbound probe removed by washing. To adapt these probe sequences to solution-based hybridization assays we compared dual labeled PNA beacons and dsPNA probes (Fig. 1). For initial comparison of dsPNA and PNA beacons we used a simple bulk fluid assay of 100 μl volume. Probe solution and bacterial culture were directly mixed and the bacteria thermolysed and incubated to allow probe hybridization. Immediately after incubation fluorescence was measured to assess probe binding. This straightforward detection protocol does not require nucleic acid purification, washing steps, or amplification and was designed to account for constraints imposed by integrated diagnostic devices for POC detection.

Comparison of PNA beacon and dsPNA probe specificity and sensitivity

To confirm probe binding and determine the appropriate probe concentration for pathogen detection, beacon or dsPNA probes ranging from 25 to 200 nM were tested for fluorescence detection of *E. coli* and *P. aeruginosa*. The highest overall fluorescence signal was achieved with the highest concentration of probe with both beacon and dsPNA probes targeting either *E. coli* (Fig. 2A) or *P. aeruginosa* (data not shown). However, the background fluorescence without bacteria remained relatively constant as the beacon concentration was increased resulting in a modestly higher fluorescence signal (Fig. 2A) and signal-to-background ratio at the highest probe concentration tested (Fig. 2B). Whereas with the dsPNA the background fluorescence increased with probe concentration, subsequently the highest signal over background was achieved at the lowest probe concentration. This suggests that a lower probe concentration could be used with the dsPNA to achieve more sensitive detection.

In many assays, probe specificity is controlled by optimizing hybridization buffer conditions such as formamide or salt concentration and by the stringency of wash conditions. However, for integration in devices with solution-based hybridization, we aimed to identify probes that were species specific in universal buffer conditions. The probe sequences used in this were found to be species specific when used as single label PNA probes in FISH assays that included stringent washing steps. Further, sequence analysis indicates these probes bind to unique sequences in 16S rRNA. Thus, we examined whether the probes retained species-specificity in the beacon and dsPNA forms in a solution-based assay without washing steps. We compared the ability of probes designed to *E. coli* and

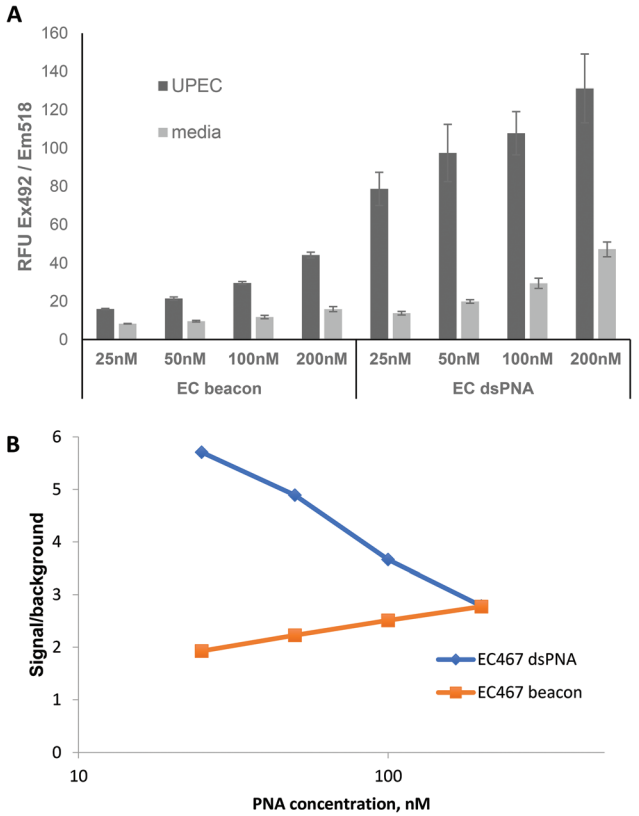

Fig. 2 Effect of probe concentration on uropathogenic *E. coli* (UPEC) detection. Fluorescent signal (A) and signal to background ratio (B) for detection of 2 × 10^8 cfu ml^{-1} UPEC with varying concentrations of EC467 PNA beacon or dsPNA with 3-fold excess quencher probe.

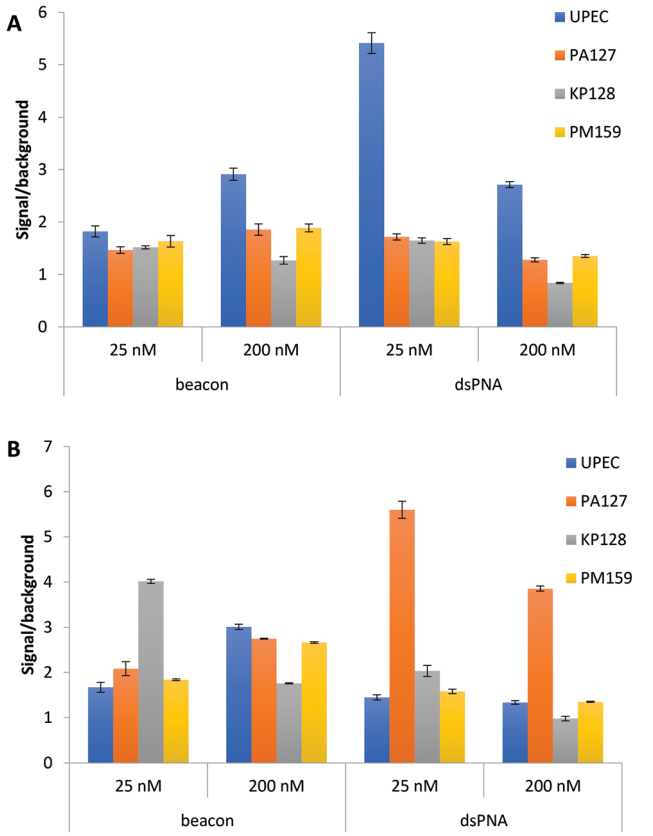

Fig. 3 Comparison of PNA beacon and dsPNA probe specificity. 200 nM or 25 nM PNA beacon or dsPNA targeting *E. coli* (EC467, A) or *P. aeruginosa* (PA584, B) was assayed for detection of the *E. coli* (UPEC), *P. aeruginosa* (Pa127), *K. pneumoniae* (Kp128), *and P. mirabilis* (Pm159).

P. aeruginosa in PNA beacon and dsPNA configurations to discriminate between uropathogenic *E. coli* (UPEC), *P. aeruginosa* (Pa127), *P. mirabilis* (Pm159), and *K. pneumoniae* (Kp128) strains. The *E. coli* targeting probe preferentially bound to *E. coli* in both conformations however the signal differential between target and other species was greatest for the dsPNA at both 25 and 200 nM probe concentrations (Fig. 3). On the other hand, the dsPNA designed to target *P. aeruginosa* showed appropriate specificity, but the beacon targeting the same sequence appeared non-specific in our assay with false positive signal from *K. pneumoniae*.

To expand our probe library beyond targeting *E. coli* and *P. aeruginosa*, we designed additional dsPNA probes for detection and classification a broader panel of pathogens. We adapted 16S rRNA probe sequences for dsPNA detection for universal eubacterial detection (UNI339), classification of *Enterobacteriaceae* (EB1272), and *Proteus mirabilis* (PM) based on previous reports.[42,44] We focused on development of dsPNA probes because they had better specificity than the beacons. To confirm specificity of all of the dsPNA probes we tested them against a broad panel of Gram negative human pathogens. Using the simple heat lysis and direct detection protocol, all of the probes exhibited the expected specificity (Fig. 4, primary data in ESI Fig. 1†). The universal probe was positive with all bacteria tested, the EB probe detected all bacteria except *P. aeruginosa*, the only non-*Enterobacteriaceae* species in the testing panel, and the EC, PA and PM probes were only positive for their appropriate target species.

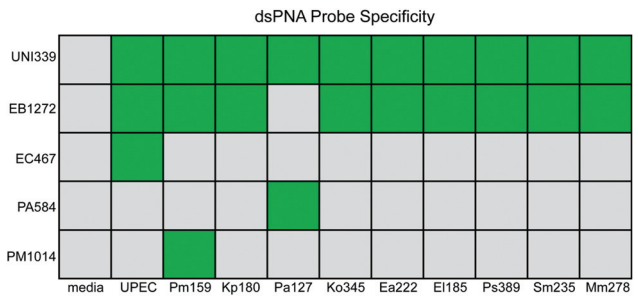

Fig. 4 Specificity of a dsPNA probes with expanded panel of pathogens. Green squares indicate positive signals with probes targeting all bacteria (UNI339), *Enterobacteriaceae* (EB1272), *E. coli* (EC467), *P. aeruginosa* (PA584), or *P. mirabilis* (PM1014) from bacterial cultures of *E. coli* (UPEC) *P. mirabilis* (Pm159), *Klebsiella pneumoniae* (Kp180), *Pseudomonas aeruginosa* (Pa127), *Klebsiella oxytoca* (Ko345), *Enterobacter aerogenes* (Ea222), *Enterobacter cloacae* (El185), *Providencia stuartii* (Ps389), *Serratia marcesens* (Sm235) or *Morganella morganii* (Mm278).

Sensitivity of detection in a relevant concentration range to the target is essential for pathogen detection. As with the specificity assay, we compared sensitivity of the PNA beacon and dsPNA a 100 μl bulk assay. Both the *E. coli* and *P. aeruginosa* targeting dsPNA probes had a higher signal-to-background ratio at the 25 nM concentration than the corresponding PNA beacon (Fig. 5). The sensitivity of detection in the bulk assay was about 10^7 cfu ml^{-1}, which is a much higher concentration than is found in most clinical samples (*e.g.* infected urine samples).

Detection of bacteria with single-cell sensitivity

To improve sensitivity of detection and assess our PNA probes in a clinically translatable system, we employed a droplet microfluidic platform for high-throughput single-cell analysis of pathogens (Fig. 6A). We designed a PDMS-based microfluidic droplet device that can passively co-encapsulate single bacterial cells and PNA probes into 7 pL volume droplets (Fig. 6B). A single bacterium confined in a 7 pL droplet drastically elevates the local bacterial concentration (equivalent to 1.4×10^8 cells per mL in bulk analysis) and hence the local target 16S rRNA concentration. Likewise, the significant reduction in volume facilitates an equivalent reduction in assay background, yielding an overall increase in signal to background ratio compared to bulk measurements. After single-bacteria encapsulation during droplet generation, droplets are transported through 95 °C and 60 °C regions to simulate the appropriate lysis and hybridization conditions as the bulk assay. Finally, the droplets pass through a flow constriction where each droplet can be measured sequentially using a custom laser-induced fluorescence (LIF) system. As droplets individually traverse the detection constriction of our microfluidic device, we register a corresponding peak in the fluorescence time trace. Droplets containing probes hybridized to their corresponding target produce higher fluorescence signal than empty droplets or droplets without target.

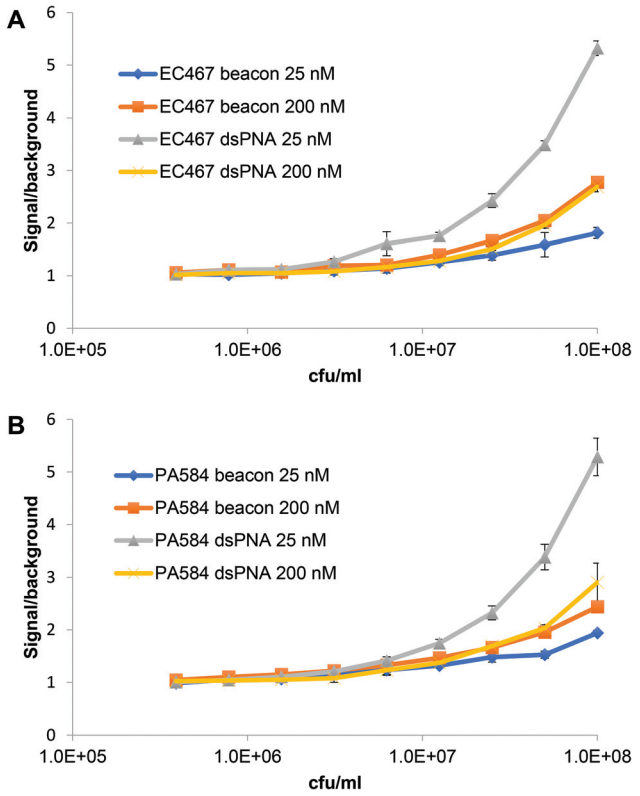

Fig. 5 Comparison of PNA beacon and dsPNA probe sensitivity. 25 and 200 nM PNA EC467 beacon or EC467 dsPNA targeting *E. coli* was used to detect varying concentrations of *E. coli* (A) or *P. aeruginosa* (B).

We used our droplet platform to test the performance of PNA beacon and dsPNA probes in detecting single pathogenic cells. We co-flowed PNA beacon or dsPNA probes as well as *E. coli* (ATCC 25922) suspended in Mueller-Hinton broth through our device and generated droplets containing *E. coli* cells and PNA probes. Following passage through the lysis and hybridization zones, the droplets were sequentially detected using the LIF system. Fig. 6Ci shows the time trace of fluorescence of droplets with *E. coli* and PNA beacon. Two populations, droplets containing the hybridized probe–target complex (green in Fig. 6Ci) and empty droplets containing no target but only the self-quenching probes (orange in Fig. 6Ci), were observed. Notably, the reduction in fluorescence background facilitated by droplets allows us to detect differentiable signal from droplets containing individual bacterial cells. This capability of our platform to detect single-bacterial cells can therefore allow for improved limit of detection for bacterial enumeration. From the resulting droplet fluorescence data for each condition, a histogram of droplet fluorescence intensity was plotted (Fig. 6Ci and 6Cii). Gaussian curve fitting was used to define a threshold 3 standard deviations above the mean of the empty droplet population (40). After analyzing ~1 000 000 droplets, the average ratio of signal from bacteria-containing droplets to signal from empty droplets ("S/B") was determined to be ~2.2. Similarly, when detecting bacteria using dsPNA probes, not only was the average signal from bacteria-containing droplets much higher, but the average S/B for bacterial detection was ~3.4, outperforming the PNA beacon.

Stronger fluorescence signals and higher S/B result in more accurate bacterial quantitation when using dsPNA probes. In our droplet experiments, we aimed to encapsulate single bacterial cells in ~10% of droplets (mean occupancy $\lambda = 0.1$). When detecting single-bacteria using the PNA beacon, after 30 min of hybridization, the rate of observed positive (observed $\lambda \approx 0.01$) droplets is much less than the rate of expected positive droplets (expected $\lambda = 0.1$). This implies that 30 min was insufficient for all the positive droplets to develop signal. In contrast, for dsPNA, the rate of observed positive droplets (observed $\lambda \approx 0.08$) more closely matches the rate of expected bacteria containing droplets. We note that the slight disagreement in mean occupancy here may have resulted from an inaccurate estimation of the initial bacterial concentration (determined *via* plating) or from a misestimation of droplet volume. However, it is clear that due to the high S/B achieved with dsPNA probes, better quantitation of single-bacteria is possible after as little as 30 min of hybridization. While these experi-

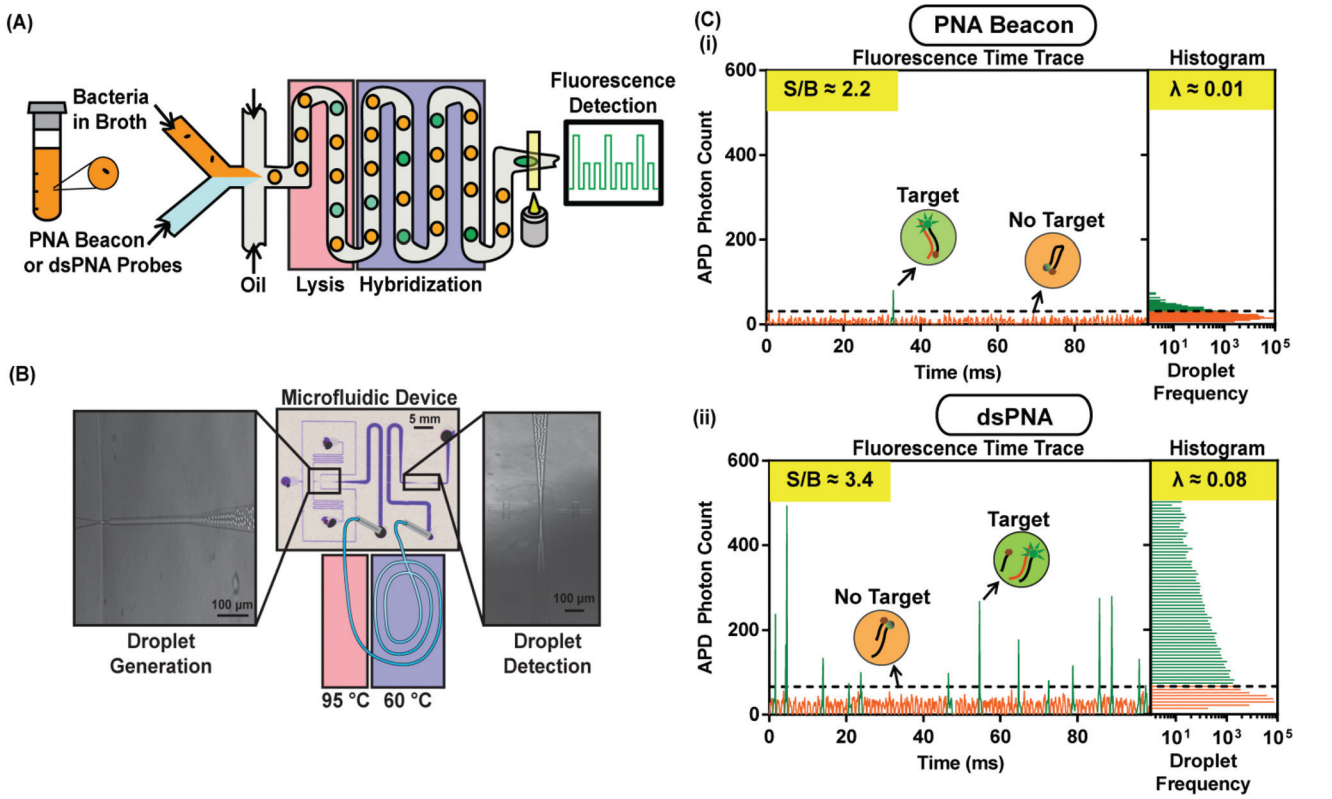

Fig. 6 Single-bacteria detection sensitivity with PNA probes using a droplet microfluidic device. (A) Single bacteria are encapsulated with either PNA beacon or dsPNA probes into 7 pL droplets. Droplets flow through a lysis region for 2 min, followed by a hybridization region for 30 min, and finally a fluorescence detection region where each droplet is individually interrogated. (B) Our PDMS-based microfluidic device consists of a droplet generation region, after which droplets are transported through 95 °C and 60 °C heaters for lysis and hybridization before re-entering the device for detection. (C) Fluorescence time trace of *E. coli* detected using (i) PNA beacon show that droplets containing target rRNA have higher fluorescence than empty droplets containing quenched probes. Here, we observe an average S/B of 2.2 and underquantification after histogram analysis, whereas when using (ii) dsPNA probes, we observe a higher S/B of 3.4 and more accurate quantification.

ments demonstrate the superiority of the dsPNA probe in detecting single *E. coli* cells in a fairly complex media (Mueller-Hinton broth), we also observed superior S/B and accurate quantitation using dsPNA probes for bacteria suspended in a simpler salt solution (hybridization buffer, data not shown).

Discussion

Highly sensitive and specific probe–target hybridization lies at the core of molecular diagnostics for infectious disease applications where there are considerable unmet needs. Rational target selection and probe design enable direct hybridization and obviate sample preparation steps including washing and target amplification, thereby facilitating translation towards POC applications. PNA-based probes offer numerous advantages compared to DNA and are well suited for direct applications using clinical samples. In this study, we compared different PNA probe configurations for direct detection of bacterial pathogens involved in common infections including urinary tract, blood stream, and surgical site. While both PNA beacon and dsPNA probes are amenable to solution-based hybridization, we found that dsPNA probes outperformed the PNA beacon of the same sequence in regard to analytical sensitivity and specificity. The performance characteristics of the dsPNA was first demonstrated in bulk fluid assays and then confirmed in a pL-droplet microfluidic platform, suggesting that our results are generalizable to many different systems.

While PNA probes are more costly and more challenging to synthesize compared to DNA probes, they offer the advantages of improved stability and hybridizations kinetics over DNA counterparts. Additionally, previous reports comparing DNA and PNA beacons for detection of *E. coli* 16S rRNA found the PNA beacon to be significantly more sensitive than the DNA beacon. PNA beacon at 50 nM bound purified RNA in the range of 0.4 to 25 nM, whereas the DNA beacon could only detect the RNA at the highest concentration.[46] With approximately 20 000 copies of rRNA per cells, 0.4 nM translates to roughly 10^7 cfu ml^{-1}, consistent with *E. coli* detection with the PNA beacon in our current study. We found a further increase in sensitivity from the beacon to the dsPNAs. dsPNA probes have also been used in some FISH based assays such as QuickFish (OpGen).[47–49] Their success with FISH using dsPNA

probes is similar to droplets in that the small encapsulation of the cell increases the effective concentration of rRNA. In a 10 pL droplet the rRNA concentration from a single bacterial cell is about 5 nM and for FISH assays the single cell rRNA concentration is even higher. The sensitivity of both FISH and droplet assays benefits from the high effective local concentration, however the current FISH assays require more hands-on steps than the droplet assay. For FISH, the bacteria are fixed and permeabilized on a microscope slide, then incubated with probe and examined microscopically, whereas in the droplet platform all assay steps and detection are automated.

While rRNA is a good target for species identification due to high cellular concentration and well-characterized sequences, conserved sequences between species necessitate high probe specificity to distinguish pathogens. Probes for solution-based diagnostics directly using biological sample ideally would retain specificity without the need to adjust salt or wash conditions. PNA probes are less sensitive to salt concentrations due to the neutral backbone and both beacon and dsPNA probes should eliminate the need for washing steps.[18] However, we found poor specificity in the beacon configuration compare to the dsPNA. This may be due in part to beacon hybridization to small stretches of homology resulting in partial opening of the probe (Table 1). Whereas in the dsPNA an excess of the quencher strand allows for competitive binding where only the full sequence can dislodge the quencher.

Quantitative detection of rRNA can be used in antibiotic susceptibility testing (AST) assays.[25] As such the dsPNA probes developed here have the potential to be used in a combined pathogen identification and AST assay by comparing fluorescence intensity with and without antibiotic. Further, the probe-based pathogen identification and AST could be adapted for use in a droplet microfluidic system. Other reports of AST in droplet systems have used resazurin as a nonspecific reporter of cell growth,[40,50] replacing resazurin with rRNA specific probes would allow for species identification and may improve analysis of polymicrobial samples.

The advantages of the dsPNA probes for bulk fluid and droplet microfluidic assays may translate well to other *in vitro* detection systems, however for some applications beacons may be more suitable. Beacons have been successfully used for dynamic intracellular nucleic acid localization in live cells.[51–54] Initial live cell imaging studies with DNA beacons found that the presence of nucleases in some cells resulted in false positive signals, but the use of PNAs and other nuclease resistant DNA modifications solved this problem.[51,55,56] In our current dsPNA design the quencher sequence is a DNA oligonucleotide and thus may require further modification for use in live cells. However, most nucleases require divalent cations as cofactors for activity and are inhibited by chelators such as EGTA. For *in vitro* diagnostics the addition of EGTA, as we have included in our assays, should inhibit nucleases and favor use of the double stranded probes.

While the hybridization characteristics of the dsPNA probes likely will remain favorable for use in a wide variety assays, this study has several limitations. Here we tested detection of a sampling of Gram negative bacterial species, yet for use in a diagnostic platform the probe panel would have to be expanded for detection of more diverse species. Additionally, the simple heat lysis used here for the Gram negative bacteria may not be robust for Gram positive species or yeast due to the thicker cell walls of these species, therefore the cell lysis would likely need to be modified to allow automated detection. A critical measure for development of these probes will be direct testing of clinical samples. The background fluorescence from biological samples may interfere with probe detection and set requirement for higher overall signal. Thus, increasing the probe concentration for different devices could allow for a balance between the need for higher signals to overcome the background of a biological sample and improved signal to noise in low background samples. Alternatively, using fluorophores with less potential for background from biological samples such as near infrared dyes may allow for robust detection directly from biological samples.

Conclusion

We have demonstrated that dsPNA probes have better specificity and sensitivity than the equivalent PNA beacon in our homogenous assays. Through testing in bulk and droplet microfluidic assays we conclude that the dsPNA is a superior choice for incorporation into a microfluidic device.

Conflicts of interest

There are no conflicts to declare.

Acknowledgements

This work was supported by the National Institutes of Health R01 1AI117032 to THW, PKK and JCL.

References

1 A. Galar, J. Leiva, M. Espinosa, F. Guillen-Grima, S. Hernaez and J. R. Yuste, *J. Infect.*, 2012, **65**, 302–309.
2 A. F. Veesenmeyer, J. A. Olson, A. L. Hersh, C. Stockmann, K. Korgenski, E. A. Thorell, A. T. Pavia and A. J. Blaschke, *Infect. Dis. Ther.*, 2016, **5**, 555–570.
3 K. K. Perez, R. J. Olsen, W. L. Musick, P. L. Cernoch, J. R. Davis, L. E. Peterson and J. M. Musser, *J. Infect.*, 2014, **69**, 216–225.
4 F. P. Maurer, M. Christner, M. Hentschke and H. Rohde, *Infect. Dis. Rep.*, 2017, **9**, 6839.
5 E. L. Tsalik, E. Petzold, B. N. Kreiswirth, R. A. Bonomo, R. Banerjee, E. Lautenbach, S. R. Evans, K. E. Hanson, J. D. Klausner, R. Patel and the Diagnostics Devices

Committee of the Antibacterial Resistance Leadership Group, *Clin. Infect. Dis.*, 2017, **64**, S41–S47.
6 A. M. Caliendo, D. N. Gilbert, C. C. Ginocchio, K. E. Hanson, L. May, T. C. Quinn, F. C. Tenover, D. Alland, A. J. Blaschke, R. A. Bonomo, K. C. Carroll, M. J. Ferraro, L. R. Hirschhorn, W. P. Joseph, T. Karchmer, A. T. MacIntyre, L. B. Reller, A. F. Jackson and A. Infectious Diseases Society of, *Clin. Infect. Dis.*, 2013, **57**(Suppl. 3), S139–S170.
7 D. R. Call, *Crit. Rev. Microbiol.*, 2005, **31**, 91–99.
8 P. L. Quan, T. Briese, G. Palacios and W. Ian Lipkin, *Antiviral Res.*, 2008, **79**, 1–5.
9 M. Bercovici, G. V. Kaigala, K. E. Mach, C. M. Han, J. C. Liao and J. G. Santiago, *Anal. Chem.*, 2011, **83**, 4110–4117.
10 A. C. Yu, G. Vatcher, X. Yue, Y. Dong, M. H. Li, P. H. Tam, P. Y. Tsang, A. K. Wong, M. H. Hui, B. Yang, H. Tang and L. T. Lau, *Front. Med.*, 2012, **6**, 173–186.
11 S. Yang and R. E. Rothman, *Lancet Infect. Dis.*, 2004, **4**, 337–348.
12 K. E. Mach, P. K. Wong and J. C. Liao, *Trends Pharmacol. Sci.*, 2011, **32**, 330–336.
13 S. M. Yoo and S. Y. Lee, *Trends Biotechnol.*, 2016, **34**, 7–25.
14 S. Tyagi and F. R. Kramer, *Nat. Biotechnol.*, 1996, **14**, 303–308.
15 Q. Li, G. Luan, Q. Guo and J. Liang, *Nucleic Acids Res.*, 2002, **30**, E5.
16 D. Meserve, Z. Wang, D. D. Zhang and P. K. Wong, *Analyst*, 2008, **133**, 1013–1019.
17 J. Zheng, R. Yang, M. Shi, C. Wu, X. Fang, Y. Li, J. Li and W. Tan, *Chem. Soc. Rev.*, 2015, **44**, 3036–3055.
18 B. Hyrup and P. E. Nielsen, *Bioorg. Med. Chem.*, 1996, **4**, 5–23.
19 P. E. Nielsen, M. Egholm, R. H. Berg and O. Buchardt, *Science*, 1991, **254**, 1497–1500.
20 M. Egholm, O. Buchardt, L. Christensen, C. Behrens, S. M. Freier, D. A. Driver, R. H. Berg, S. K. Kim, B. Norden and P. E. Nielsen, *Nature*, 1993, **365**, 566–568.
21 V. V. Demidov, V. N. Potaman, M. D. Frank-Kamenetskii, M. Egholm, O. Buchard, S. H. Sonnichsen and P. E. Nielsen, *Biochem. Pharmacol.*, 1994, **48**, 1310–1313.
22 U. Giesen, W. Kleider, C. Berding, A. Geiger, H. Orum and P. E. Nielsen, *Nucleic Acids Res.*, 1998, **26**, 5004–5006.
23 H. Stender, M. Fiandaca, J. J. Hyldig-Nielsen and J. Coull, *J. Microbiol. Methods*, 2002, **48**, 1–17.
24 E. Altobelli, R. Mohan, K. E. Mach, M. L. Sin, V. Anikst, M. Buscarini, P. K. Wong, V. Gau, N. Banaei and J. C. Liao, *Eur. Urol. Focus*, 2017, **3**, 293–299.
25 K. E. Mach, R. Mohan, E. J. Baron, M. C. Shih, V. Gau, P. K. Wong and J. C. Liao, *J. Urol.*, 2011, **185**, 148–153.
26 S. Bakshi, A. Siryaporn, M. Goulian and J. C. Weisshaar, *Mol. Microbiol.*, 2012, **85**, 21–38.
27 H. Bremer and P. P. Dennis, *EcoSal Plus*, 2008, **3**, DOI: 10.1128/ecosal.5.2.3.
28 P. C. Woo, S. K. Lau, J. L. Teng, H. Tse and K. Y. Yuen, *Clin. Microbiol. Infect.*, 2008, **14**, 908–934.
29 F. O. Glockner, P. Yilmaz, C. Quast, J. Gerken, A. Beccati, A. Ciuprina, G. Bruns, P. Yarza, J. Peplies, R. Westram and W. Ludwig, *J. Biotechnol.*, 2017, **261**, 169–176.
30 J. R. Cole and J. M. Tiedje, *RNA Biol.*, 2014, **11**, 239–243.
31 J. R. Cole, Q. Wang, J. A. Fish, B. Chai, D. M. McGarrell, Y. Sun, C. T. Brown, A. Porras-Alfaro, C. R. Kuske and J. M. Tiedje, *Nucleic Acids Res.*, 2014, **42**, D633–D642.
32 H. Frickmann, A. E. Zautner, A. Moter, J. Kikhney, R. M. Hagen, H. Stender and S. Poppert, *Crit. Rev. Microbiol.*, 2017, **43**, 263–293.
33 A. Moter and U. B. Gobel, *J. Microbiol. Methods*, 2000, **41**, 85–112.
34 K. Churski, T. S. Kaminski, S. Jakiela, W. Kamysz, W. Baranska-Rybak, D. B. Weibel and P. Garstecki, *Lab Chip*, 2012, **12**, 1629–1637.
35 T. S. Kaminski, O. Scheler and P. Garstecki, *Lab Chip*, 2016, **16**, 2168–2187.
36 A. Kaushik, K. Hsieh and T. Wang, *WIREs Nanomed. Nanobiotechnol.*, 2018, **10**, e1522.
37 V. Taly, D. Pekin, A. El Abed and P. Laurent-Puig, *Trends Mol. Med.*, 2012, **18**, 405–416.
38 H. Zec, D. J. Shin and T. H. Wang, *Expert Rev. Mol. Diagn.*, 2014, **14**, 787–801.
39 D. K. Kang, M. M. Ali, K. Zhang, S. S. Huang, E. Peterson, M. A. Digman, E. Gratton and W. Zhao, *Nat. Commun.*, 2014, **5**, 5427.
40 A. M. Kaushik, K. Hsieh, L. Chen, D. J. Shin, J. C. Liao and T. H. Wang, *Biosens. Bioelectron.*, 2017, **97**, 260–266.
41 T. D. Rane, H. C. Zec, C. Puleo, A. P. Lee and T. H. Wang, *Lab Chip*, 2012, **12**, 3341–3347.
42 R. I. Amann, B. J. Binder, R. J. Olson, S. W. Chisholm, R. Devereux and D. A. Stahl, *Appl. Environ. Microbiol.*, 1990, **56**, 1919–1925.
43 S. Malic, K. E. Hill, A. Hayes, S. L. Percival, D. W. Thomas and D. W. Williams, *Microbiology*, 2009, **155**, 2603–2611.
44 R. Mohan, K. E. Mach, M. Bercovici, Y. Pan, L. Dhulipala, P. K. Wong and J. C. Liao, *PLoS One*, 2011, **6**, e26846.
45 H. Perry-O'Keefe, S. Rigby, K. Oliveira, D. Sorensen, H. Stender, J. Coull and J. J. Hyldig-Nielsen, *J. Microbiol. Methods*, 2001, **47**, 281–292.
46 C. Xi, M. Balberg, S. A. Boppart and L. Raskin, *Appl. Environ. Microbiol.*, 2003, **69**, 5673–5678.
47 M. K. Deck, E. S. Anderson, R. J. Buckner, G. Colasante, J. M. Coull, B. Crystal, P. Della Latta, M. Fuchs, D. Fuller, W. Harris, K. Hazen, L. L. Klimas, D. Lindao, M. C. Meltzer, M. Morgan, J. Shepard, S. Stevens, F. Wu and M. J. Fiandaca, *J. Clin. Microbiol.*, 2012, **50**, 1994–1998.
48 M. K. Deck, E. S. Anderson, R. J. Buckner, G. Colasante, T. E. Davis, J. M. Coull, B. Crystal, P. D. Latta, M. Fuchs, D. Fuller, W. Harris, K. Hazen, L. L. Klimas, D. Lindao, M. C. Meltzer, M. Morgan, J. Shepard, S. Stevens, F. Wu and M. J. Fiandaca, *Diagn. Microbiol. Infect. Dis.*, 2014, **78**, 338–342.
49 H. Salimnia, M. R. Fairfax, P. Lephart, M. Morgan, J. J. Gilbreath, S. M. Butler-Wu, K. E. Templeton,

F. J. Hamilton, F. Wu, R. Buckner, D. Fuller, T. E. Davis, A. M. Abdelhamed, M. R. Jacobs, A. Miller, B. Pfrommer and K. C. Carroll, *J. Clin. Microbiol.*, 2014, **52**, 3928–3932.

50 L. Jiang, L. Boitard, P. Broyer, A. C. Chareire, P. Bourne-Branchu, P. Mahe, M. Tournoud, C. Franceschi, G. Zambardi, J. Baudry and J. Bibette, *Eur. J. Clin. Microbiol. Infect. Dis.*, 2016, **35**, 415–422.

51 T. Kuang, L. Chang, X. Peng, X. Hu and D. Gallego-Perez, *Trends Biotechnol.*, 2017, **35**, 347–359.

52 R. Monroy-Contreras and L. Vaca, *J Nucleic Acids*, 2011, **2011**, 741723.

53 B. M. Wile, K. Ban, Y. S. Yoon and G. Bao, *Nat. Protoc.*, 2014, **9**, 2411–2424.

54 H. Y. Yeh, M. V. Yates, A. Mulchandani and W. Chen, *Proc. Natl. Acad. Sci. U. S. A.*, 2008, **105**, 17522–17525.

55 A. K. Chen, M. A. Behlke and A. Tsourkas, *Nucleic Acids Res.*, 2007, **35**, e105.

56 Z. Ma, X. Wu, C. J. Krueger and A. K. Chen, *Genomics, Proteomics Bioinf.*, 2017, **15**, 279–286.

